

*Letter to the Editor***Preliminary results on the circumstellar envelopes of α Ori and R Leo from CO 4.6 μm line emission**N. Ryde¹, B. Gustafsson¹, K.H. Hinkle², K. Eriksson¹, D.L. Lambert³, and H. Olofsson⁴¹ Uppsala Astronomical Observatory, Box 515, S-751 20, Uppsala, Sweden² National Optical Astronomy Observatories*, P.O. Box 26732, Tucson, AZ 85726, USA³ Department of Astronomy, University of Texas, Austin, TX 78712, USA⁴ Stockholm Observatory, S-133 36 Saltsjöbaden, Sweden

Received 7 May 1999 / Accepted 15 June 1999

Abstract. CO 4.6 μm vibration-rotational lines are detected in fluorescent emission from the inner regions of the Betelgeuse (α Orionis) and R Leonis stellar winds. The spatially and spectrally resolved 1-0 R(1), R(2), and R(3) line profiles are found to be highly useful probes of circumstellar shells. The current data sample only a few regions of the circumstellar shells of the program stars. However, now it should be possible to obtain envelope maps and absolute flux estimates, allowing new independent estimates of mass loss rates. This will open up new possibilities in the study of the structure and dynamics of stellar winds around red giants. The temperature 4'' away from α Ori is found to be 38^{+6}_-5 K. For R Leo the temperature 4'' North is derived to be 24^{+3}_-2 K and 4'' South 35^{+7}_-4 K.

Key words: stars: AGB and post-AGB – stars: circumstellar matter – stars: individual: α Ori – stars: individual: R Leo – stars: late-type – infrared: stars

1. Introduction

Envelopes around late-type giants have been studied systematically in various ways. These include molecular microwave line observations, visual observations of atomic or molecular resonance lines along the line of sight to the stellar photosphere, and mapping the IR continuum emission due to dust. Among the most powerful techniques for exploring these shells are imaging techniques. Spectral line imaging has been carried out at millimetre wavelengths. An equivalent approach in the visual spectrum is to map atomic resonance scattering of photospheric light in the shell. Bernat & Lambert bernat:75 carried out pioneering observations of α Ori in the K1 resonance line. Since then, more than ten stellar envelopes have been explored in this way by various groups (e.g. Gustafsson et al. 1997).

Send offprint requests to: N. Ryde (nils.ryde@astro.uu.se)

* Operated by the Association of Universities for Research in Astronomy, Inc. under cooperative agreement with the National Science Foundation

A first attempt to use the infrared line spectrum to map a circumstellar shell in resonance scattering was made by Wannier & Sahai sahai:85. They reported observations of the CO fundamental lines in the bright, dust-enshrouded star CW Leo. By observing infrared vib-rot CO lines in combination with millimetre CO lines, it is possible to compare infrared CO data from the inner wind regions with CO millimetre data originating in the outer regions (cf. Ryde et al. 1999). This could give clues to the temporal development of the CO envelope and allow comparison of the CO morphology at different distances from the star. Wannier and Sahai observed the circumstellar shell through an annulus and thus produced only spatially averaged information. They found that the mass loss rate in the inner parts of the circumstellar shell was less than that in the region observed in the millimetre CO lines.

Since the Wannier and Sahai observations great advances have been made in infrared detectors. However, the application of infrared arrays in high resolution spectroscopy is not simple since at wavelengths longer than about 1.6 μm thermal radiation from room temperature spectrographs dominates the stellar signals. Application of these arrays to line-resolved spectroscopy involves building cryogenic spectrographs. A high resolution ($\lambda/\Delta\lambda \sim 10^5$) spectrograph of this type, which is much more sensitive than previous infrared spectrometers, has recently been completed at Kitt Peak National Observatory (Hinkle et al. 1998). In this *letter* we present the first attempts to map the CO shells in IR of the bright M1-supergiant α Ori and the M8-giant R Leo. These stars have been selected due to their large circumstellar shells and large radial velocities, to provide the conditions necessary for the stellar CO-lines to be shifted out of the telluric ones. A geocentric radial velocity of at least 20–30 km s^{-1} is required.

2. Observations and reductions

The observations were carried out on 1997, March 27 with the 2.1 meter telescope at Kitt Peak using Phoenix, a cryogenic echelle spectrograph. Phoenix is a long-slit high spec-

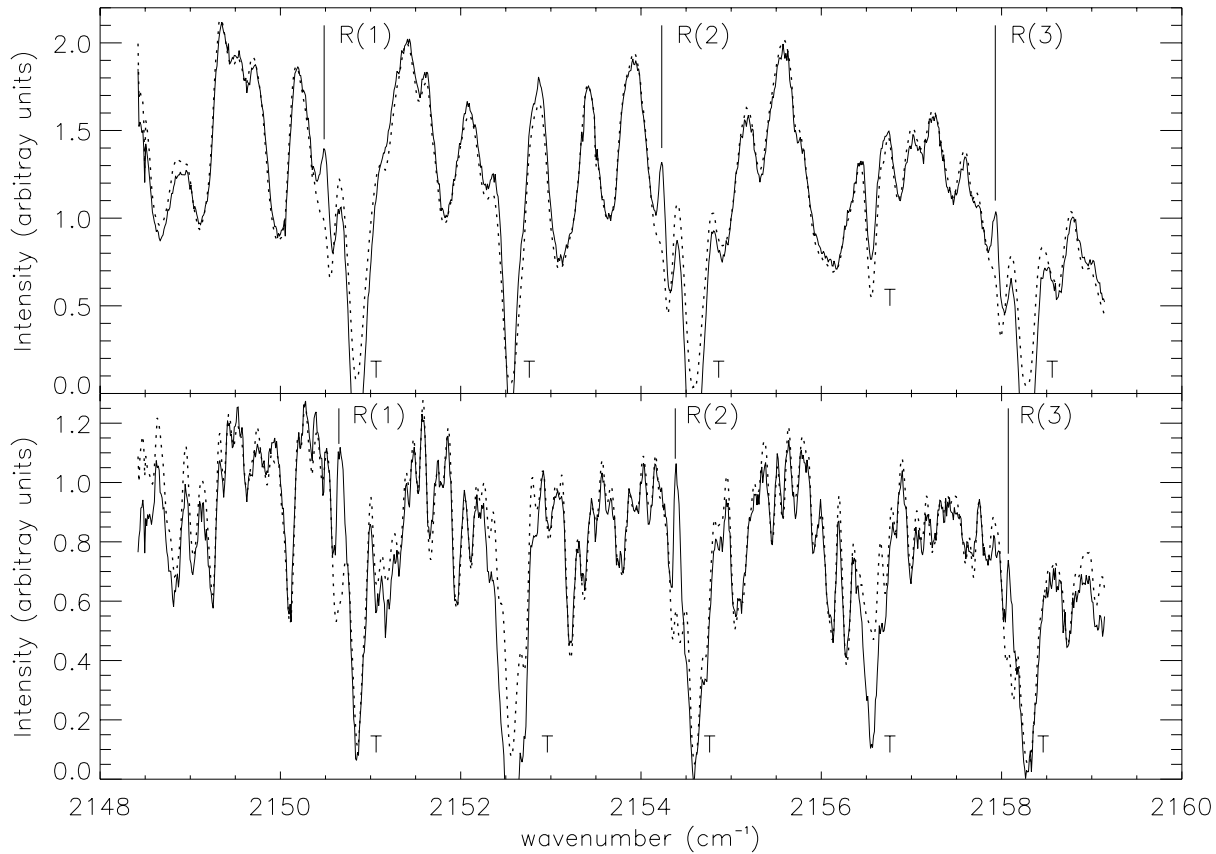


Fig. 1. Above, the spectrum of α Ori (Betelgeuse) and below the spectrum of R Leo with the abscissa showing the wavenumber scale of the observer. The solid line is the off-star spectrum and the dotted line is an appropriately scaled on-star spectrum. The three circumstellar CO vib-rot emission lines, which are marked with R(1), R(2), and R(3) ‘fill in’ the corresponding on-star lines which are in absorption. To the right (blue) of these lines their telluric counterparts are seen. The major telluric lines are denoted with a capital T. During the time between the exposure of the off-star spectrum and the corresponding background exposure, the telluric lines may change. This is the reason why the telluric lines in the off-star spectra can be negative

tral resolution infrared spectrograph designed for the 1–5 μm region (Hinkle et al. 1998). For our observations, we employed a 1.4'' wide (4-pixel-wide) by 50'' long entrance slit. We achieved a spectral resolution of $R \sim 40,000$ ($\approx 7.5 \text{ km s}^{-1}$ or 0.054 cm^{-1} at 2150 cm^{-1}). The inverse linear dispersion is $8.86 \times 10^{-3} \text{ cm}^{-1}/\text{pixel}$, which means that the observed spectrum is over-sampled. The spatial imaging (along the direction of the slit) was fairly poor for this set of observations. In 1997 Phoenix suffered from both coma and astigmatism in the collimator as the result of an incorrectly mounted mirror. When the collimator was focused for best spectral resolution, significant spatial blurring resulted. The resulting spatial resolution along the slit was about $\sim 6''$ and as a result spatial information along the slit was of limited value and not used in this project. Also, the slit could not be rotated from a fixed east-west orientation. We chose a grating setting for observing low excitation lines of the vib-rot fundamental R-branch of $^{12}\text{C}^{16}\text{O}$. The lines selected, 1-0 R(1), 1-0 R(2), and 1-0 R(3) (2150.86 , 2154.60 , and 2158.30 cm^{-1}), have minimal interference with telluric lines. Spectral coverage is limited by the array length of 1024 pixels; we observed the region 2149 to 2159 cm^{-1} .

The thermal sky-background infrared radiation will be large and somewhat variable. Phoenix is not a sky balanced device, which means that the thermal radiation is recorded. The thermal sky radiation would limit exposure times to about ten minutes. However, many of the telluric lines are optically thick and are seen in emission. To avoid saturation of these lines, exposures were limited to 60 seconds. In order to remove the thermal spectrum from the stellar spectrum, the telescope was nodded between the source and a region of sky, and the sky exposure was subtracted from the source exposure (cf. Joyce 1992). Since Phoenix has a long slit, nodding along the slit is possible. Observations both on and off the star were obtained. As the program stars were bright, the exposure time on these objects was only ten seconds. For off-star observations nods were from the off-star position to a position an additional $25''$ off the star. The off-star exposures were sums of ten 60 second exposures. During a ten minute interval the sky background level is quite constant and the airmass changes by only a few percent. Array pixel sensitivity differences were removed using flats and darks as described by Joyce joyce.

The on-star intensity is typically about six times brighter than the sky background. The emission searched for is around

150 times weaker than the on-star intensity. The off-star spectra were taken with the slit 4'' North (both stars) and South (R Leo only) of the star. Due to the limited spectral range, the cold off-star spectrum included only the R(1), R(2), and R(3) emission lines of ^{12}CO , except for the scattered stellar light. The on-star spectrum was normalised to unit level and then scaled to the off-star level. The circumstellar CO vib-rot emission is obtained by subtracting the scaled on-star spectrum from the off-star, Fig. 2.

A velocity shift compared to the ‘telluric wavelength scale’ is determined from several of the identified photospheric lines. The heliocentric velocity derived from this shift for α Ori is $24.1 \pm 1.9 \text{ km s}^{-1}$ and for R Leo it is $13.6 \pm 1.9 \text{ km s}^{-1}$. Both velocities are in excellent agreement with the values given in the literature (cf. GCRV, Wilson 1953) which is a reassuring test of the wavenumber scale.

These observations are the first to be made using this method with the Phoenix spectrometer. Future observations with the same instrumentation, adjusted to give a higher spatial resolution, will provide envelope maps of spatial resolution limited by the seeing.

3. Analysis and results

We have succeeded in detecting circumstellar CO-vib-rot lines in emission at 4.6 μ m around the supergiant α Ori and the M-type Mira R Leo. In Fig. 1 the off-star spectra of α Ori and R Leo are shown. Superimposed are the on-star spectra, which are scaled by an appropriate constant factor in order to match the overall structure of the off-star spectra. The emission of the stellar wind is clearly seen. The wavelength scale is that of the observer. The off-star spectrum is built up of two parts. Firstly, the stellar light is scattered in the Earth’s atmosphere, the telescope, the spectrometer, and/or by dust grains in the circumstellar shell. This will lead to a spectrum resembling the on-star one. Secondly, the CO vib-rot emission lines are superimposed. The molecules are radiatively excited by the stellar light and the subsequent decay produces an emission line. In Fig. 1 the telluric lines are also marked. The 2152.5 and 2156.5 cm^{-1} telluric lines are from water vapour. During the observing night the weather was changing and as a result conspicuous changes in the on-star and off-star strengths of these lines can be seen. The varying telluric lines illustrate the need to use only stellar lines shifted outside the telluric CO emission. With the help of the Arcturus Infrared Atlas (Hinkle et al. 1995), nearly all features in the spectra are identified as coming from photospheric ^{12}CO and ^{13}CO . High vibrational transitions are seen, implying a photospheric origin.

The broadening of the photospheric lines in the spectrum of the supergiant α Ori is about four times as large as in the spectrum of the giant R Leo, most likely a consequence of a velocity broadening, possibly due to large convective eddies.

The kinetic gas temperatures of envelopes of AGB-stars are difficult to measure (Rodgers & Glassgold 1991). Bernat et al. 1979 used observations of α Ori at 4.6 μ m to show that for the vibrational ground level of CO the radiative rates are only some percent of the collisional rates, implying an LTE

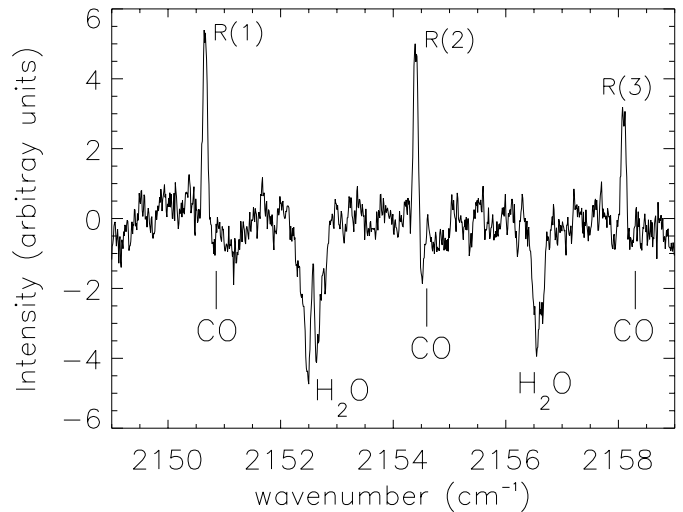


Fig. 2. An example of a subtracted spectrum (see text); in this case the emission spectrum 4'' North of R Leo. The telluric lines are indicated in the lower part of the figure. The telluric water lines usually vary more and faster than the telluric CO lines. In this spectrum the telluric CO lines have not changed very much, whereas the water lines have varied more between the on-star and the off-star exposures. When subtracting the two spectra, the telluric lines can either go below or over zero depending how they have varied. From the amplitude of the CO emission lines and the noise (which includes both photon noise and spurious mismatch between on-star and off-star spectra, cf. Fig. 1) we estimate a S/N of at least 5

situation for the ground level. The excitation temperature determined from the ground level of CO is therefore the kinetic temperature. The emission in the winds is due to de-excitations of radiatively excited states of the second vibrational state. From the equations of statistical equilibrium for the lowest states of the two first vibrational levels, it is possible to derive the following equation for the ratio of the intensities of the vib-rot lines R(1) and R(3), $I_{R(1)}/I_{R(3)}$ and similarly for $I_{R(2)}/I_{R(3)}$. In the derivation one may neglect higher vibrational levels since $v=1$ is poorly populated in comparison to $v=0$. Here, we assume that the vibrational ground state is in rotational LTE (Bernat et al. 1979). Furthermore, the assumption is made that the mean intensity of the radiation exciting the CO molecules in the wind is constant over the narrow frequency range considered and that the lines are optically thin. We find

$$\frac{I_{R(1)}}{I_{R(3)}} = \frac{\nu_1 A_{21} (A_{45} + A_{43}) (3 \cdot B_{12} e^{-2\gamma} + 7 \cdot B_{32} e^{-12\gamma})}{\nu_3 A_{43} (A_{23} + A_{21}) (7 \cdot B_{34} e^{-12\gamma} + 11 \cdot B_{54} e^{-30\gamma})}, \quad (1)$$

with $\gamma = Bhc/(kT)$, where the rotational constant, B , for the vibrational ground state of CO is 1.9225 cm^{-1} . $A_{J',J''}$ and $B_{J',J''}$ are the Einstein coefficients for spontaneous emission and absorption for the fundamental transitions with the rotational quantum numbers as subscripts. The Einstein coefficients were calculated from tables of the absorption oscillator strengths (Kirby-Docken & Liu 1978, which for our lines are consistent with Huré & Roueff 1996). This equation provides a possibility

Table 1. Observed circumstellar CO vib-rot line ratios for α Ori and R Leo. Derived model temperatures using Eq. 1 are also given

Object	Line Ratio	4'' North	Temp.	4'' South	Temp.
α Ori	$I_{R(1)}/I_{R(3)}$	1.17	39 K		
	$I_{R(2)}/I_{R(3)}$	1.25	36 K		
R Leo	$I_{R(1)}/I_{R(3)}$	1.78	24 K	1.12	41 K
	$I_{R(2)}/I_{R(3)}$	1.57	24 K	1.40	29 K

to determine the kinetic temperature of the emitting molecules. The emissions from the R(1), R(2) and R(3) lines are measured by subtracting the fitted on-star spectrum from the off-star one. The latter is observed approximately (4_{-1}^{+3})'' North of α Ori. In this way the ratios $I_{R(1)}/I_{R(3)}$ and $I_{R(2)}/I_{R(3)}$ are retrieved and these will provide two different measurements of the temperature via the model above, see Table 1. The mean of these measurements is for α Ori 38 K, with an estimated error of about 5 K. The error is estimated by measuring extrema in integrated fluxes, with the noise taken in account (Fig. [2]).

A model of α Ori (Rodgers & Glassgold 1991), which is based on the thermal balance of the envelope, including adiabatic and line cooling and dust-drag heating, suggests a temperature of 37 K at a distance of 4'' away from the star with a slow temperature dependence on distance, $T \propto r^{-1/2}$. Our value of the temperature, which is in good agreement with the value given by this model, is a mean of the kinetic temperatures along the line of sight, but also a spatial mean due to the seeing and the spatial degradation due the collimator problem.

For R Leo the excitation temperature (4_{-1}^{+3})'' North is derived to be 24_{-2}^{+3} K and (4_{-1}^{+3})'' South to be 35_{-4}^{+7} K, the errors being estimated measuring uncertainties. The derived temperatures based on Eq. (1) are valid only on the assumption that the vibrational ground level is in rotational LTE. This requires such high densities that sufficiently large numbers of collisions take place to be able to set up a Boltzmann distribution. If this is not the case, the two line ratios will not necessarily give two consistent temperatures. This could be the case for R Leo.

Based on the reasoning in Gustafsson et al. bg:97 it is possible to estimate the distance, or the ‘impact parameter’ p , from the star where the optical depth is unity in the line-of-sight. Beyond this distance a steady homogeneous wind can be considered to be optically thin. The impact parameter for the R(1) transition of the CO fundamental is (cf. Eq. (9) in Gustafsson et al. [1997]) $p_{\tau=1}[\text{cm}] \sim 1.9 \times 10^{28} \cdot N_3(\text{CO})/N(\text{CO}) \cdot N(\text{CO})/N(\text{H}) \cdot M(\text{M}_{\odot}\text{yr}^{-1})/v_e^2(\text{km s}^{-1})$. For α Ori, which has a $M = 2.0 \times 10^{-6} \text{M}_{\odot} \text{yr}^{-1}$, $N(\text{CO})/N(\text{H}) = 2.6 \times 10^{-5}$ (Huggins et al. 1994) and $v_e = 13.6 \text{ km s}^{-1}$ (Loup et al. 1993), the impact parameter is $p_{\tau=1} = 1.6 \times 10^{15} \text{ cm}$, which corresponds to 0''.8 for α Ori at a distance of 131 pc (ESA 1997). Here, we have assumed, as a mean, that 30% of the CO molecules are excited to the $J=2$ -level, $N_3(\text{CO})/N(\text{CO}) \sim 0.3$. R Leo has a mass-loss rate of $\dot{M} = 1.1 \times 10^{-7} \text{M}_{\odot} \text{yr}^{-1}$ (scaled to the distance as measured by the Hipparcos satellite [ESA 1997]), $N(\text{CO})/N(\text{H}) = 4 \times 10^{-4}$ (Bujarrabal et al. 1989), and a terminal expansion velocity of $v_e = 8.5 \text{ km s}^{-1}$ (Loup

et al. 1993). This leads for R Leo at a distance of 101 pc to $p_{\tau=1} = 3.5 \times 10^{15} \text{ cm}$, corresponding to 2''.3. Thus, both winds should, if homogeneous, be optically thin at 4''.

4. Discussion and conclusion

We have succeeded in detecting CO vib-rot lines in emission at 4.6 μ m around the supergiant α Ori and the M-type Mira R Leo. The relative strengths of the different lines for α Ori suggest a temperature in the envelope of about 37 K at a distance of $\sim 4''$ from the star, in agreement with current model estimates. For R Leo similar temperatures are estimated at distances of $\sim 4''$ from the star, with some possibilities of a non-isotropic temperature distribution. These temperature estimates are based on the assumption that the vibrational ground state is in rotational LTE, and that the lines are optically thin, which is also suggested by a simple model.

Instrumental problems decreased severely the spatial resolution of the observations and a real mapping of the envelopes, as was planned, could not be made. In future observations special efforts must be made to secure exact positioning of the slit, high accuracy in the wavelength and flux calibration, good focusing, etc. Then, with the current instrumentation, it should be possible to obtain envelope maps, as well as absolute flux estimates which will enable independent, new estimates of mass-loss rates to be made. There are good reasons to believe that the CO lines, as studied by the Phoenix spectrometer, will open up a number of interesting new possibilities in the study of the structure and dynamics of stellar winds around red giants.

Acknowledgements. We thank the referee for valuable comments and J. Barnes, Drs. P. Barklem, R. Joyce, S. Ridgeway, and N. Piskunov for enlightening discussions. This research was supported by the Swedish National Space Board and the Swedish Natural Science Research Council.

References

- Bernat A. P., Hall D. N. B., Hinkle K. H., Ridgway S. T., 1979, *ApJ* 233, L135
- Bernat A. P., Lambert D. L., 1975, *ApJ* 201, L153
- Bujarrabal V., Gomez-Gonzales J., Planesas P., 1989, *A&A* 219, 256
- ESA, 1997, *The Hipparcos and Tycho Catalogues*, ESA SP-1200
- Gustafsson B., Eriksson K., Kiselman D., Olander N., Olofsson H., 1997, *A&A* 318, 535
- Hinkle K., Wallace L., Livingston W., 1995, *PASP* 107, 1042
- Hinkle K. H., Cuberly R. W., Gaughan N. A., et al., 1998, *SPIE* 3354, 810
- Huggins P. J., Bachiller R., Cox P., Forveille T., 1994, *ApJ* 424, L127
- Hur  J. M., Roueff E., 1996, *A&AS* 117, 561
- Joyce R. R., 1992, in S. Howell (ed.), *ASP Conf. Ser.* 23, *Astronomical CCD Observing and Reduction Tech.*, p. 258
- Kirby-Docken K., Liu B., 1978, *ApJS* 36, 359
- Loup C., Forveille T., Omont A., Paul J., 1993, *A&AS* 99, 291
- Rodgers B., Glassgold A. E., 1991, *ApJ* 382, 606
- Ryde N., Sch oier F. L., Olofsson H., 1999, *A&A* 345, 841
- Sahai R., Wannier P. G., 1985, *ApJ* 299, 424
- Wilson R. E., 1953, *Carnegie Inst. Washington D.C. Publ.* 601